Since January 2020 Elsevier has created a COVID-19 resource centre with free information in English and Mandarin on the novel coronavirus COVID-19. The COVID-19 resource centre is hosted on Elsevier Connect, the company's public news and information website.

Nanoluciferase-based cell fusion assay for rapid and high-throughput assessment of SARS-CoV-2-neutralizing antibodies in patient samples

Max Meyrath[a,b], Martyna Szpakowska[a], Jean-Marc Plesseria[a], Olivia Domingues[a], Jérémie Langlet[c], Bernard Weber[b], Rejko Krüger[d,e,f], Markus Ollert[a,g,†], and Andy Chevigné[a,*,†] on behalf of the CON-VINCE Consortium

[a]Department of Infection and Immunity, Luxembourg Institute of Health (LIH), Esch-sur-Alzette, Luxembourg
[b]Laboratoires Réunis Luxembourg, Z.A.C. Laangwiss, Junglinster, Luxembourg
[c]Business Development Office, Luxembourg Institute of Health (LIH), Strassen, Luxembourg
[d]Transversal Translational Medicine (TTM), Luxembourg Institute of Health (LIH), Strassen, Luxembourg
[e]Luxembourg Centre for Systems Biomedicine (LCSB), University of Luxembourg, Esch-Belval, Luxembourg
[f]Centre Hospitalier de Luxembourg (CHL), Luxembourg, Luxembourg
[g]Department of Dermatology and Allergy Center, Odense Research Center for Anaphylaxis, Odense University Hospital, University of Southern Denmark, Odense, Denmark
*Corresponding author: e-mail address: andy.chevigne@lih.lu

Contents

† These authors contributed equally to this work.

Methods in Enzymology
ISSN 0076-6879
https://doi.org/10.1016/bs.mie.2022.07.015

Abstract

After more than two years, COVID-19 still represents a global health burden of unprecedented extent and assessing the degree of immunity of individuals against SARS-CoV-2 remains a challenge. Virus neutralization assays represent the gold standard for assessing antibody-mediated protection against SARS-CoV-2 in sera from recovered and/or vaccinated individuals. Neutralizing antibodies block the interaction of viral spike protein with human angiotensin-converting enzyme 2 (ACE2) receptor *in vitro* and prevent viral entry into host cells. Classical viral neutralization assays using full replication-competent viruses are restricted to specific biosafety level 3-certified laboratories, limiting their utility for routine and large-scale applications. We developed therefore a cell-fusion-based assay building on the interaction between viral spike and ACE2 receptor expressed on two different cell lines, substantially reducing biosafety risks associated with classical viral neutralization assays. This chapter describes this simple, sensitive, safe and cost-effective approach for rapid and high-throughput evaluation of SARS-CoV-2 neutralizing antibodies relying on high-affinity NanoLuc® luciferase complementation technology (HiBiT). When applied to a variety of standards and patient samples, this method yields highly reproducible results in 96-well, as well as in 384-well format. The use of novel NanoLuc® substrates with increased signal stability like Nano-Glo® Endurazine™ furthermore allows for high flexibility in assay set-up and full automatization of all reading processes. Lastly, the assay is suitable to evaluate the neutralizing capacity of sera against the existing spike variants, and potentially variants that will emerge in the future.

1. Introduction

In February 2020, the World Health Organization (WHO) declared the outbreak of Severe Acute Respiratory Syndrome Coronavirus type 2 (SARS-CoV-2) causing Coronavirus Disease 2019 (COVID-19) as a pandemic (Cucinotta & Vanelli, 2020). As of May 2022, SARS-CoV-2 has infected over 500 million people and caused over 6 million deaths, with over 1 million in the US alone (https://coronavirus.jhu.edu/). Structurally, SARS-CoV-2 is a typical betacoronavirus with a nucleoprotein-encapsidated positive-sense RNA genome surrounded by a lipid bilayer from which large spike glycoproteins (S) protrude (Chan et al., 2020; Li et al., 2020). Spike protein forms homotrimers consisting of S1 and S2 subunits and exists in a metastable prefusion conformation. S1 subunit comprises a globular head domain containing the receptor-binding domain (RBD), responsible for virus binding to cell surface receptor angiotensin-converting enzyme 2

(ACE2) (Hoffmann et al., 2020; Walls et al., 2020; Wrapp et al., 2020). Once bound to its receptor, spike protein undergoes large conformational changes, activating the fusogenic potential of S2 subunit and ultimately allowing viral entry into the host cell (Huang, Yang, Xu, Xu, & Liu, 2020; Walls et al., 2017). It is mainly against the spike protein that naturally produced and therapeutic neutralizing antibodies are targeted, with the RBD being immunodominant, but not the only immunogenic region (Du, Yang, & Zhang, 2021; Liu et al., 2020; Piccoli et al., 2020; Wajnberg et al., 2020).

Numerous studies could show that although natural infection and vaccination provide a robust protection against SARS-CoV-2 infection, antibody titers appear to rapidly decline over time and the same level of protection is no longer guaranteed after several months (Gaebler et al., 2021; Israel et al., 2021; Vacharathit et al., 2021). Limited protection over time is even more pronounced for new emerging variants with reduced antibody neutralization profile like Omicron variant (Dejnirattisai et al., 2022; Meng et al., 2022; Zou et al., 2022). Hence, despite a high vaccination coverage in many countries, accurate monitoring of the population to assess their degree of immune protection against the virus and its different variants remains crucial (Snoeck et al., 2020; Wilmes et al., 2021).

Since the beginning of the pandemic, standard serological assays allowed to quickly detect the presence of virus-specific antibodies (IgM, IgA or IgG), indicative of an ongoing or past infection. However, they do not allow to infer the anti-viral protection of these antibodies, as these antibodies may lack neutralizing properties. Determining the amount of neutralizing antibodies (NAbs) therefore provides more reliable information on the protection of an individual or a population.

Different types of assays to measure the presence of NAbs have been reported since decades for various kinds of viruses, including coronaviruses (Cai et al., 2016; Krah, Amin, Nalin, & Provost, 1991; Sarzotti-Kelsoe et al., 2014; Sehr et al., 2013; Zhu et al., 2007). The development of assays for these pathogens and their applicability to routine or high-throughput format is a challenge and many aspects including sensitivity, stability, run-to-run reproducibility and biosafety issues must be taken into account.

First, unmodified virus can be propagated *in vitro* on susceptible cell lines, enabling to determine a biologic's neutralizing potency by plaque reduction neutralization tests (PRNT) and microneutralization tests (MNT) (Bewley et al., 2021; Deshpande et al., 2020; Rockx et al., 2008). Although considered as the gold standard for measuring levels of virus-neutralizing

antibodies, this kind of long and fastidious assay is not compatible with high-throughput measurements and its use is limited to BSL-3 facilities. Alternatively, pseudotyped-viruses (pseudoviruses) which are chimeric viruses consisting of a core surrounded by an envelope bearing surface glycoproteins from a donor virus are widely used in lower biosafety facilities (BSL-2) as substitutes for highly infectious viruses. For SARS-CoV-1, MERS-CoV and SARS-CoV-2, the cell entry-mediating S proteins were successfully displayed on replication-defective pseudoviruses derived from Moloney murine leukemia virus (MuLV) (Han, Kim, Kim, Poon, & Cho, 2004), human immunodeficiency virus type 1 (HIV-1) (Zhao et al., 2013) or vesicular stomatitis virus (VSV) (Almahboub, Algaissi, Alfaleh, ElAssouli, & Hashem, 2020; Case et al., 2020; Nie et al., 2020), respectively. Such an approach also allows to use a wide range of reporter genes including β-galactosidase, luciferase or green fluorescent protein (GFP) facilitating biophysical and more reproducible readouts. Although pseudoviruses are a valuable alternative for BSL3-restricted replication-competent viruses, they do have some limitations. For example, it is hard to predict whether the incorporated glycoprotein is presented in its correct conformation and adequately processed form on a pseudovirus. Moreover, the amount of surface glycoproteins per pseudoviral particle might greatly vary between production batches and between particles within one batch, thus not accurately mimicking the infectivity and neutralization profile of the virus of interest and making it difficult to standardize the assay between laboratories.

Cell-free neutralization assays to monitor SARS-CoV-2 neutralizing antibodies have also been developed like for example those commercialized by Meso Scale Diagnostics (Johnson et al., 2020) or Promega (Janaka, Clark, Evans, & Connor, 2021). Several other non-commercialized cell-free assays have furthermore been described (Danh et al., 2020; Fenwick et al., 2021; Mravinacova et al., 2022). Although these assays show low biosafety risk and applicability to high-throughput formats, they may suffer from limitations linked to the use of proteins in a non-native context. Indeed, both spike proteins and/or ACE2 receptors may show an incorrect conformation as they are not integrated in a functional cellular membrane and sometimes only RBD or monomeric spike rather than the entire trimeric protein are used.

Surface proteins from many different viruses are able to induce membrane fusion, and assays building on virus-cell or cell-cell fusion to screen

for antibodies or inhibitors have been established for several viruses, including SARS-CoV-1 (Herschhorn et al., 2011; Marin et al., 2015; Sha et al., 2006; York & Nunberg, 2018). It quickly became clear that SARS-CoV-2 can similarly induce spike-mediated syncytia formation (Buchrieser et al., 2021) and with an even higher efficiency than SARS-CoV-1, probably due to an optimized furin cleavage site (Hornich et al., 2021; Jaimes, Millet, & Whittaker, 2020; Xia et al., 2020). It should be noted that efforts have already been launched to develop a SARS-CoV-2 antibody neutralization assay based on cell-cell fusion using split GFP, β-galactosidase complementation or HIV Tat transactivation of a firefly luciferase gene as readout (Saunders et al., 2022; Theuerkauf et al., 2021; Zhao et al., 2021). However, to our knowledge, so far no assay has been built on the complementation of the ultra-bright last generation NanoLuc® luciferase, which is more suitable for high-throughput applications, given the excellent repeatability, run-to-run reproducibility and signal-to-noise ratio even in small-volume formats (Luís et al., 2022; Palmer et al., 2022).

NanoLuc® is a small (19 kDa) engineered luciferase capable of efficient, ATP-independent light emission using stable Furimazine as substrate, with biochemical and physical characteristics superior to the commonly used bioluminescence-producing enzymes (Hall et al., 2012). NanoLuc® luminescence activity is approximately 100-fold greater than classical luciferases such as Firefly (Fluc, 61 kDa) and Renilla (Rluc, 36 kDa) luciferases, allowing to work with low volumes and high-throughput format such as 384-well plates. Moreover, optimized NanoLuc® substrates like Nano-Glo® Endurazine™ and Vivazine™ are now available and enable live-cell, non-lytic assays lasting several hours or even days. The development of two complementation partners with extremely high affinity (pM range) toward each other (HiBiT technology (Dixon et al., 2016)) allows for extraordinarily efficient reconstitution of the full NanoLuc® upon cell fusion and a great signal-to-noise ratio.

Here, we describe in detail the materials and protocols for this simple and safe cell-cell fusion assay for rapid and high-throughput evaluation of SARS-CoV-2 neutralizing antibodies relying on high-affinity NanoLuc® complementation technology (HiBiT). We provide examples of its power in terms of high-throughput applicability, reproducibility in 96-well and 384-well format, as well as assay flexibility in regard to extended readout time and characterization of different circulating spike variant.

2. Before you begin

This virus-free assay uses two cell lines expressing respectively the viral spike and host cell receptor ACE2 on their surface and builds on the principle that cell membranes merge upon spike-ACE2 interaction. Each cell line additionally expresses one part of the NanoLuc® luciferase (HiBiT or LgBiT) that on their own do not emit light, but when brought together, quickly self-complement due to their high affinity for each other to reconstitute a fully functional NanoLuc® (HiBiT technology, Promega). When co-incubated, these two cell lines are able to form syncytia through their cell membrane fusion facilitated by the spike-ACE2 interaction, in turn allowing rapid and spontaneous complementation of the cytoplasmic NanoLuc® fragments and giving rise to ultra-bright bioluminescence in the presence of a specific substrate (Fig. 1). Similar to classical viral neutralization assays, pre-incubation with neutralizing antibodies blocking the spike-ACE2 interaction prevents syncytia formation, which can be titrated and quantified by measuring the reduced light emission in comparison to cells that were not treated with neutralizing antibodies (Fig. 1A and C).

Using the material, vectors and protocols described below, this "SARScytium" assay can easily and reproducibly be performed using transiently transfected cells, where one cell line is transfected with viral spike and LgBiT, whereas the other cell line is transfected with HiBiT and ACE2 (Fig. 1A). The approach using transient transfections allows for high versatility and flexibility of the assay with easy and fast adaptability to spike variants. This can be of particular interest given that the antibody neutralization profile considerably varies between the different spike variants and the high probability of emergence of new variants (Duarte et al., 2022; Harvey et al., 2021). Alternatively, cells stably expressing the required proteins can be used. This accounts especially for ACE2, where a variety of cells stably expressing ACE2 are commercially available, such as Vero E6 cells that endogenously express ACE2, or HEK or HeLa cells exogenously overexpressing ACE2 together or not with the protease TMPRSS2 that serves as a co-factor for SARS-CoV-2 infection and is implicated in spike priming on the membrane.

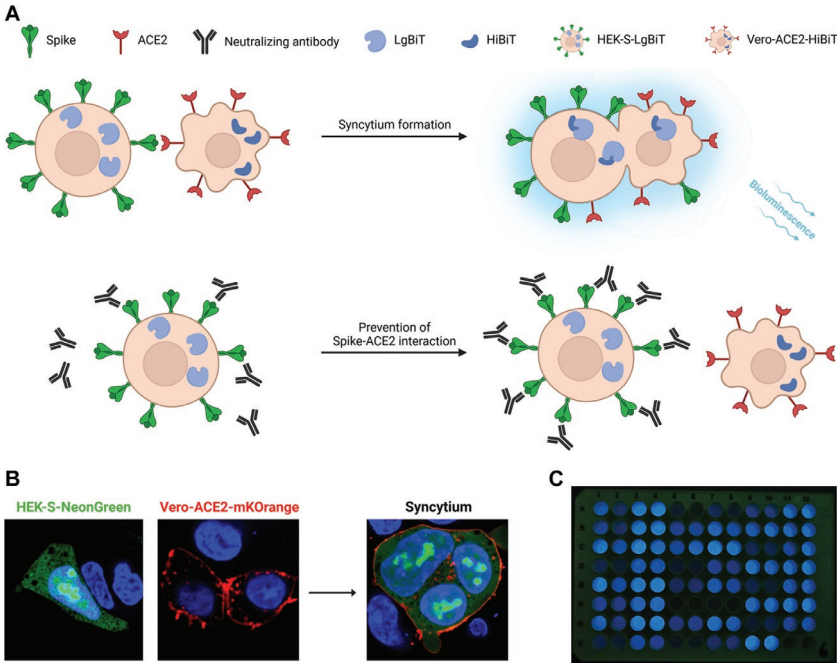

Fig. 1 Cell fusion assay based on high-affinity NanoLuc® complementation (HiBiT) (A) Schematic representation of the assay set-up. LgBiT and spike-expressing HEK293T cells are mixed with HiBiT- and ACE2-expressing Vero E6 cells and co-incubated overnight. Upon spike interaction with ACE2, cell membranes merge, forming a multinucleated syncytium and enabling complementation of both NanoLuc® fragments, eventually leading to light emission upon substrate addition. Pre-incubation of spike-expressing cells with neutralizing antibodies will prevent the spike–ACE2 interaction and limit syncytia formation. Multiple sera can be tested simultaneously in 96- or 384-well format, enabling high-throughput screening of samples. (B) Representative microscopy pictures, illustrating syncytium formation between Vero E6 cells expressing an mKOrange-tagged membrane marker and HEK293T cells expressing a NeonGreen cytoplasmic marker. DAPI-stained nuclei are depicted in blue. (C) Representative picture of a 96-well plate after substrate addition taken with an ordinary mobile phone camera (Huawei p20 Pro). The intense blue bioluminescent signal emitted by the NanoLuc® is well visible even with the naked eye. No light is emitted from wells where cells did not efficiently form syncytia, indicative of the presence of neutralizing antibodies. *Panel A: Figure was created using BioRender.com.*

3. Materials and equipment

3.1 Cell culture and transfection

- Cell culture flasks (Greiner Bio-One)
- Dulbecco's modified Eagle medium (DMEM, GIBCO) supplemented with 0.04 mM phenol red, 1 mM sodium pyruvate, 4 mM L-glutamine, 4.5 g/L glucose, supplemented with 10% fetal bovine serum (FBS, Merck) and 100 units/mL of penicillin and 100 μg/mL of streptomycin (GIBCO)
- 10-cm cell culture dishes (Corning)
- Opti-MEM, Reduced Serum Medium (GIBCO)
- Polyethylenimine (PEI, 1 mg/mL, Merck)
- LgBiT expression construct
- HiBiT expression construct
- SARS-CoV-2 spike protein expression construct
- Human embryonic kidney 293T (HEK293T) cells (for example CRL-3216, ATCC)
- Vero E6 cells (for example CoronaGrow-VeroE6, CL0001, VectorBuilder)

See section below for amino acid sequences of protein expression constructs.

3.1.1 Alternatives

Note that the choice of appropriate cell lines is crucial to guarantee efficient syncytium formation. Instead of Vero E6 cells, other cell lines such as HEK cells stably overexpressing human ACE2 receptor (for example CoronaAssay-293T (hACE2-hTMPRSS2, CL0015, VectorBuilder) can be considered. However in our hands, although these cells allowed efficient syncytia formation, neutralization assays using spike-specific antibodies were generally less efficient. This was probably due to the abundant ACE2 expression levels, allowing syncytium formation even with low amounts of available/non-neutralized spike protein. ACE2 expression on cell surface can for example be verified by flow cytometry using the ACE2-specific antibody AF933 (R&D systems).

Similarly, alternatives for the spike-expressing HEK293T cells might be considered. We obtained comparable results using for example HeLa cells, whereas almost no syncytium formation was detected using U-87

MG glioblastoma or Chinese Hamster Ovary (CHO) cells, likely due to a lack of required cofactors or membrane proteases in these cell lines.

3.2 Sample preparation and bioluminescence reading

- Phosphate-buffered saline (PBS)
- Versene (0.48 mM EDTA in PBS, GIBCO)
- 15-mL conical centrifuge tube (Greiner Bio-One)
- White flat-bottom LUMITRAC 96-well plates, medium binding (Greiner Bio-One)
- Transparent U-bottom 96-well plates (Greiner Bio-One)
- 12-channel pipets: 2–20 μL range and 20–200 μL range (Mettler Toledo)
- CASY Automated cell counter (OMNI Life Science)
- NanoLuc® substrate: Furimazine (Nano-Glo® Live Cell Assay System, Promega), Nano-Glo® Vivazine™ or Endurazine™ (Promega) or Coelenterazine H (Regis Technologies)
- Luminescence plate reader (GloMax Explorer, Promega)

3.3 Sequences of NanoLuc® partners and spike expression constructs

3.3.1 HiBiT

MVSGWRLFKKIS

3.3.2 LgBiT

MVFTLEDFVGDWEQTAAYNLDQVLEQGGVSSLLQNLAVSVTPIQ
RIVRSGENALKIDIHVIIPYEGLSADQMAQIEEVFKVVYPVDDHHF
KVILPYGTLVIDGVTPNMLNYFGRPYEGIAVFDGKKITVTGTLWN
GNKIIDERLITPDGSMLFRVTIN

3.3.3 Spike variants

See note 3a and 3b

3.3.4 Spike (WT)

MFVFLVLLPLVSSQCVNLTTRTQLPPAYTNSFTRGVYYPDKVFRS
SVLHSTQDLFLPFFSNVTWFHAIHVSGTNGTKRFDNPVLPFNDGV
YFASTEKSNIIRGWIFGTTLDSKTQSLLIVNNATNVVIKVCEFQFC

NDPFLGVYYHKNNKSWMESEFRVYSSANNCTFEYVSQPFLMDLE
GKQGNFKNLREFVFKNIDGYFKIYSKHTPINLVRDLPQGFSALEP
LVDLPIGINITRFQTLLALHRSYLTPGDSSSGWTAGAAAYYVGYLQ
PRTFLLKYNENGTITDAVDCALDPLSETKCTLKSFTVEKGIYQTS
NFRVQPTESIVRFPNITNLCPFGEVFNATRFASVYAWNRKRISNC
VADYSVLYNSASFSTFKCYGVSPTKLNDLCFTNVYADSFVIRGDE
VRQIAPGQTGKIADYNYKLPDDFTGCVIAWNSNNLDSKVGGNYN
YLYRLFRKSNLKPFERDISTEIYQAGSTPCNGVEGFNCYFPLQSYGF
QPTNGVGYQPYRVVVLSFELLHAPATVCGPKKSTNLVKNKCVNF
NFNGLTGTGVLTESNKKFLPFQQFGRDIADTTDAVRDPQTLEILD
ITPCSFGGVSVITPGTNTSNQVAVLYQDVNCTEVPVAIHADQLTP
TWRVYSTGSNVFQTRAGCLIGAEHVNNSYECDIPIGAGICASYQ
TQTNSPRRARSVASQSIIAYTMSLGAENSVAYSNNSIAIPTNFTISV
TTEILPVSMTKTSVDCTMYICGDSTECSNLLLQYGSFCTQLNRAL
TGIAVEQDKNTQEVFAQVKQIYKTPPIKDFGGFNFSQILPDPSKPS
KRSFIEDLLFNKVTLADAGFIKQYGDCLGDIAARDLICAQKFNGLT
VLPPLLTDEMIAQYTSALLAGTITSGWTFGAGAALQIPFAMQMAY
RFNGIGVTQNVLYENQKLIANQFNSAIGKIQDSLSSTASALGKLQ
DVVNQNAQALNTLVKQLSSNFGAISSVLNDILSRLDKVEAEVQID
RLITGRLQSLQTYVTQQLIRAAEIRASANLAATKMSECVLGQSKR
VDFCGKGYHLMSFPQSAPHGVVFLHVTYVPAQEKNFTTAPAICH
DGKAHFPREGVFVSNGTHWFVTQRNFYEPQIITTDNTFVSGNCD
VVIGIVNNTVYDPLQPELDSFKEELDKYFKNHTSPDVDLGDISGINA
SVVNIQKEIDRLNEVAKNLNESLIDLQELGKYEQYIKWPWYIWLG
FIAGLIAIVMVTIMLCCMTSCCSCLKGCCSCGSCC*DYKDHDGDY*
KDHDIDYKDDDDK

3.3.5 Spike (alpha)

Mutations introduced: H69_V70del, Y144del, N501Y, A570D, D614G, P681H, T716I, S982A, D1118H. The entire sequence can be found here: https://cloud.lih.lu/s/ML423WRWR4z5rB7.

spike (Alpha)

MFVFLVLLPLVSSQCVNLTTRTQLPPAYTNSFTRGVYYPDKVFRSSVLHSTQDLFLPFFSNVTWFHA
I_._.SGTNGTKRFDNPVLPFNDGVYFASTEKSNIIRGWIFGTTLDSKTQSLLIVNNATNVVIKVCEFQF
CNDPFLGVY_.HKNNKSWMESEFRVYSSANNCTFEYVSQPFLMDLEGKQGNFKNLREFVFKNIDGY
FKIYSKHTPINLVRDLPQGFSALEPLVDLPIGINITRFQTLLALHRSYLTPGDSSSGWTAGAAAYYVG
YLQPRTFLLKYNENGTITDAVDCALDPLSETKCTLKSFTVEKGIYQTSNFRVQPTESIVRFPNITNLCP
FGEVFNATRFASVYAWNRKRISNCVADYSVLYNSASFSTFKCYGVSPTKLNDLCFTNVYADSFVIR
GDEVRQIAPGQTGKIADYNYKLPDDFTGCVIAWNSNNLDSKVGGNYNYLYRLFRKSNLKPFERDIS
TEIYQAGSTPCNGVEGFNCYFPLQSYGFQPT**Y**GVGYQPYRVVVLSFELLHAPATVCGPKKSTNLVK
NKCVNFNFNGLTGTGVLTESNKKFLPFQQFGRDI**D**DTTDAVRDPQTLEILDITPCSFGGVSVITPGTN
TSNQVAVLYQ**G**VNCTEVPVAIHADQLTPTWRVYSTGSNVFQTRAGCLIGAEHVNNSYECDIPIGAGI
CASYQTQTNS**H**RRARSVASQSIIAYTMSLGAENSVAYSNNSIAIP**I**NFTISVTTEILPVSMTKTSVDCT
MYICGDSTECSNLLLQYGSFCTQLNRALTGIAVEQDKNTQEVFAQVKQIYKTPPIKDFGGFNFSQILP
DPSKPSKRSFIEDLLFNKVTLADAGFIKQYGDCLGDIAARDLICAQKFNGLTVLPPLLTDEMIAQYTS
ALLAGTITSGWTFGAGAALQIPFAMQMAYRFNGIGVTQNVLYENQKLIANQFNSAIGKIQDSLSSTA
SALGKLQDVVNQNAQALNTLVKQLSSNFGAISSVLNDIL**A**RLDKVEAEVQIDRLITGRLQSLQTYVT
QQLIRAAEIRASANLAATKMSECVLGQSKRVDFCGKGYHLMSFPQSAPHGVVFLHVTYVPAQEKN
FTTAPAICHDGKAHFPREGVFVSNGTHWFVTQRNFYEPQIITT**H**NTFVSGNCDVVIGIVNNTVYDPL
QPELDSFKEELDKYFKNHTSPDVDLGDISGINASVVNIQKEIDRLNEVAKNLNESLIDLQELGKYEQY
IKWPWYIWLGFIAGLIAIVMVTIMLCCMTSCCSCLKGCCSCGSCC*DYKDHDGDYKDHDIDYKDDDD*
K

3.3.6 Spike (beta)

Mutations introduced: L18F, D80A, D215G, L242_L244del, R246I, K417N, E484K, N501Y, D614G, A701V. The entire sequence can be found here: https://cloud.lih.lu/s/wGqYNnFHHJ5DSH6.

spike (Beta)

MFVFLVLLPLVSSQCVN**F**TTRTQLPPAYTNSFTRGVYYPDKVFRSSVLHSTQDLFLPFFSNVTWFHA
IHVSGTNGTKRF**A**NPVLPFNDGVYFASTEKSNIIRGWIFGTTLDSKTQSLLIVNNATNVVIKVCEFQF
CNDPFLGVYYHKNNKSWMESEFRVYSSANNCTFEYVSQPFLMDLEGKQGNFKNLREFVFKNIDGY
FKIYSKHTPINLVR**G**LPQGFSALEPLVDLPIGINITRFQTL_._._.H**I**SYLTPGDSSSGWTAGAAAYYVG
YLQPRTFLLKYNENGTITDAVDCALDPLSETKCTLKSFTVEKGIYQTSNFRVQPTESIVRFPNITNLCP
FGEVFNATRFASVYAWNRKRISNCVADYSVLYNSASFSTFKCYGVSPTKLNDLCFTNVYADSFVIR
GDEVRQIAPGQTG**N**IADYNYKLPDDFTGCVIAWNSNNLDSKVGGNYNYLYRLFRKSNLKPFERDIS
TEIYQAGSTPCNGV**K**GFNCYFPLQSYGFQPT**Y**GVGYQPYRVVVLSFELLHAPATVCGPKKSTNLVK
NKCVNFNFNGLTGTGVLTESNKKFLPFQQFGRDIADTTDAVRDPQTLEILDITPCSFGGVSVITPGTN
TSNQVAVLYQ**G**VNCTEVPVAIHADQLTPTWRVYSTGSNVFQTRAGCLIGAEHVNNSYECDIPIGAGI
CASYQTQTNSPRRARSVASQSIIAYTMSLG**V**ENSVAYSNNSIAIPTNFTISVTTEILPVSMTKTSVDCT
MYICGDSTECSNLLLQYGSFCTQLNRALTGIAVEQDKNTQEVFAQVKQIYKTPPIKDFGGFNFSQILP
DPSKPSKRSFIEDLLFNKVTLADAGFIKQYGDCLGDIAARDLICAQKFNGLTVLPPLLTDEMIAQYTS
ALLAGTITSGWTFGAGAALQIPFAMQMAYRFNGIGVTQNVLYENQKLIANQFNSAIGKIQDSLSSTA
SALGKLQDVVNQNAQALNTLVKQLSSNFGAISSVLNDILSRLDKVEAEVQIDRLITGRLQSLQTYVT
QQLIRAAEIRASANLAATKMSECVLGQSKRVDFCGKGYHLMSFPQSAPHGVVFLHVTYVPAQEKN
FTTAPAICHDGKAHFPREGVFVSNGTHWFVTQRNFYEPQIITTDNTFVSGNCDVVIGIVNNTVYDPL
QPELDSFKEELDKYFKNHTSPDVDLGDISGINASVVNIQKEIDRLNEVAKNLNESLIDLQELGKYEQY
IKWPWYIWLGFIAGLIAIVMVTIMLCCMTSCCSCLKGCCSCGSCC*CDYKDHDGDYKDHDIDYKDDDD*
K

3.3.7 Spike (gamma)

Mutations introduced: L18F, T20N, P26S, D138Y, R190S, K417T, E484K, N501Y, D614G, H655Y, T1027I, V1176F. The entire sequence can be found here: https://cloud.lih.lu/s/jYRiMRtJdbZineb.

spike (Gamma)

MFVFLVLLPLVSSQCVN**F**T**N**RTQLP**S**AYTNSFTRGVYYPDKVFRSSVLHSTQDLFLPFFSNVTWFHA
IHVSGTNGTKRFDNPVLPFNDGVYFASTEKSNIIRGWIFGTTLDSKTQSLLIVNNATNVVIKVCEFQF
CN**Y**PFLGVYYHKNNKSWMESEFRVYSSANNCTFEYVSQPFLMDLEGKQGNFKNL**S**EFVFKNIDGY
FKIYSKHTPINLVRDLPQGFSALEPLVDLPIGINITRFQTLLALHRSYLTPGDSSSGWTAGAAAYYVG
YLQPRTFLLKYNENGTITDAVDCALDPLSETKCTLKSFTVEKGIYQTSNFRVQPTESIVRFPNITNLCP
FGEVFNATRFASVYAWNRKRISNCVADYSVLYNSASFSTFKCYGVSPTKLNDLCFTNVYADSFVIR
GDEVRQIAPGQTG**T**IADYNYKLPDDFTGCVIAWNSNNLDSKVGGNYNYLYRLFRKSNLKPFERDIS
TEIYQAGSTPCNGV**K**GFNCYFPLQSYGFQPT**Y**GVGYQPYRVVVLSFELLHAPATVCGPKKSTNLVK
NKCVNFNFNGLTGTGVLTESNKKFLPFQQFGRDIADTTDAVRDPQTLEILDITPCSFGGVSVITPGTN
TSNQVAVLYQ**G**VNCTEVPVAIHADQLTPTWRVYSTGSNVFQTRAGCLIGAE**Y**VNNSYECDIPIGAGI
CASYQTQTNSPRRARSVASQSIIAYTMSLGAENSVAYSNNSIAIPTNFTISVTTEILPVSMTKTSVDCT
MYICGDSTECSNLLLQYGSFCTQLNRALTGIAVEQDKNTQEVFAQVKQIYKTPPIKDFGGFNFSQILP
DPSKPSKRSFIEDLLFNKVTLADAGFIKQYGDCLGDIAARDLICAQKFNGLTVLPPLLTDEMIAQYTS
ALLAGTITSGWTFGAGAALQIPFAMQMAYRFNGIGVTQNVLYENQKLIANQFNSAIGKIQDSLSSTA
SALGKLQDVVNQNAQALNTLVKQLSSNFGAISSVLNDILSRLDKVEAEVQIDRLITGRLQSLQTYVT
QQLIRAAEIRASANLAA**I**KMSECVLGQSKRVDFCGKGYHLMSFPQSAPHGVVFLHVTYVPAQEKNF
TTAPAICHDGKAHFPREGVFVSNGTHWFVTQRNFYEPQIITTDNTFVSGNCDVVIGIVNNTVYDPLQ
PELDSFKEELDKYFKNHTSPDVDLGDISGINAS**F**VNIQKEIDRLNEVAKNLNESLIDLQELGKYEQYI
KWPWYIWLGFIAGLIAIVMVTIMLCCMTSCCSCLKGCCSCGSCC*DYKDHDGDYKDHDIDYKDDDDK*

3.3.8 Spike (delta)

Mutations introduced: T19R, G142D, E156_F157del, R158G, L452R, T478K, D614G, P681R, D950N. The entire sequence can be found here: https://cloud.lih.lu/s/8bW2qcpqdDL59i2.

spike (Delta)

MFVFLVLLPLVSSQCVNL**R**TRTQLPPAYTNSFTRGVYYPDKVFRSSVLHSTQDLFLPFFSNVTWFHA
IHVSGTNGTKRFDNPVLPFNDGVYFASTEKSNIIRGWIFGTTLDSKTQSLLIVNNATNVVIKVCEFQF
CNDPFL**D**VYYHKNNKSWMES_._.**G**VYSSANNCTFEYVSQPFLMDLEGKQGNFKNLREFVFKNIDG
YFKIYSKHTPINLVRDLPQGFSALEPLVDLPIGINITRFQTLLALHRSYLTPGDSSSGWTAGAAAYYV
GYLQPRTFLLKYNENGTITDAVDCALDPLSETKCTLKSFTVEKGIYQTSNFRVQPTESIVRFPNITNLC
PFGEVFNATRFASVYAWNRKRISNCVADYSVLYNSASFSTFKCYGVSPTKLNDLCFTNVYADSFVIR
GDEVRQIAPGQTGKIADYNYKLPDDFTGCVIAWNSNNLDSKVGGNYNY**R**YRLFRKSNLKPFERDIS
TEIYQAGS**K**PCNGVEGFNCYFPLQSYGFQPTNGVGYQPYRVVVLSFELLHAPATVCGPKKSTNLVK
NKCVNFNFNGLTGTGVLTESNKKFLPFQQFGRDIADTTDAVRDPQTLEILDITPCSFGGVSVITPGTN
TSNQVAVLYQ**G**VNCTEVPVAIHADQLTPTWRVYSTGSNVFQTRAGCLIGAEHVNNSYECDIPIGAGI
CASYQTQTNS**R**RRARSVASQSIIAYTMSLGAENSVAYSNNSIAIPTNFTISVTTEILPVSMTKTSVDCT
MYICGDSTECSNLLLQYGSFCTQLNRALTGIAVEQDKNTQEVFAQVKQIYKTPPIKDFGGFNFSQILP
DPSKPSKRSFIEDLLFNKVTLADAGFIKQYGDCLGDIAARDLICAQKFNGLTVLPPLLTDEMIAQYTS
ALLAGTITSGWTFGAGAALQIPFAMQMAYRFNGIGVTQNVLYENQKLIANQFNSAIGKIQDSLSSTA
SALGKLQ**N**VVNQNAQALNTLVKQLSSNFGAISSVLNDILSRLDKVEAEVQIDRLITGRLQSLQTYVT
QQLIRAAEIRASANLAATKMSECVLGQSKRVDFCGKGYHLMSFPQSAPHGVVFLHVTYVPAQEKN
FTTAPAICHDGKAHFPREGVFVSNGTHWFVTQRNFYEPQIITTDNTFVSGNCDVVIGIVNNTVYDPL
QPELDSFKEELDKYFKNHTSPDVDLGDISGINASVVNIQKEIDRLNEVAKNLNESLIDLQELGKYEQY
IKWPWYIWLGFIAGLIAIVMVTIMLCCMTSCCSCLKGCCSCGSCC*DYKDHDGDYKDHDIDYKDDDD*
K

3.3.9 Spike (Omicron)

Mutations introduced: A67V, H69_V70del, T95I, G142D, V143_Y145del, N211del, L212I, R214_D215insEPE, G339D, S371L, S373P, S375F, K417N, N440K, G446S, S477N, T478K, E484A, Q493R, G496S, Q498R, N501Y, Y505H, T547K, D614G, H655Y, N679K, P681H, N764K, D796Y, N856K, Q954H, N969K, L981F. The entire sequence can be found here: https://cloud.lih.lu/s/N9smQENLKBfA6oF.

spike (Omicron)

MFVFLVLLPLVSSQCVNLTTRTQLPPAYTNSFTRGVYYPDKVFRSSVLHSTQDLFLPFFSNVTWFHV
I_._.SGTNGTKRFDNPVLPFNDGVYFASIEKSNIIRGWIFGTTLDSKTQSLLIVNNATNVVIKVCEFQFC
NDPFLD_._._.HKNNKSWMESEFRVYSSANNCTFEYVSQPFLMDLEGKQGNFKNLREFVFKNIDGYF
KIYSKHTPI_.IVREPEDLPQGFSALEPLVDLPIGINITRFQTLLALHRSYLTPGDSSSGWTAGAAAYYV
GYLQPRTFLLKYNENGTITDAVDCALDPLSETKCTLKSFTVEKGIYQTSNFRVQPTESIVRFPNITNLC
PFDEVFNATRFASVYAWNRKRISNCVADYSVLYNLAPFFTFKCYGVSPTKLNDLCFTNVYADSFVI
RGDEVRQIAPGQTGNIADYNYKLPDDFTGCVIAWNSNKLDSKVSGNYNYLYRLFRKSNLKPFERDI
STEIYQAGNKPCNGVAGFNCYFPLRSYSFRPTYGVGHQPYRVVVLSFELLHAPATVCGPKKSTNLV
KNKCVNFNFNGLKGTGVLTESNKKFLPFQQFGRDIADTTDAVRDPQTLEILDITPCSFGGVSVITPGT
NTSNQVAVLYQGVNCTEVPVAIHADQLTPTWRVYSTGSNVFQTRAGCLIGAEYVNNSYECDIPIGA
GICASYQTQTKSHRRARSVASQSIIAYTMSLGAENSVAYSNNSIAIPTNFTISVTTEILPVSMTKTSVD
CTMYICGDSTECSNLLLQYGSFCTQLKRALTGIAVEQDKNTQEVFAQVKQIYKTPPIKYFGGFNFSQI
LPDPSKPSKRSFIEDLLFNKVTLADAGFIKQYGDCLGDIAARDLICAQKFKGLTVLPPLLTDEMIAQY
TSALLAGTITSGWTFGAGAALQIPFAMQMAYRFNGIGVTQNVLYENQKLIANQFNSAIGKIQDSLSS
TASALGKLQDVVNHNAQALNTLVKQLSSKFGAISSVLNDIFSRLDKVEAEVQIDRLITGRLQSLQTY
VTQQLIRAAEIRASANLAATKMSECVLGQSKRVDFCGKGYHLMSFPQSAPHGVVFLHVTYVPAQE
KNFTTAPAICHDGKAHFPREGVFVSNGTHWFVTQRNFYEPQIITTDNTFVSGNCDVVIGIVNNTVYD
PLQPELDSFKEELDKYFKNHTSPDVDLGDISGINASVVNIQKEIDRLNEVAKNLNESLIDLQELGKYE
QYIKWPWYIWLGFIAGLIAIVMVTIMLCCMTSCCSCLKGCCSCGSCC*DYKDHDGDYKDHDIDYKDD*
DDK

3.3.10 Fusion-deficient spike ("spike DEAD")

Mutations introduced: RRAR682-685 to AAAA, KR814-815 to GH. The entire sequence can be found here: https://cloud.lih.lu/s/3HKoT8eADiEaw4b See note 3c.

Fusion-deficient spike ("spike DEAD")

MFVFLVLLPLVSSQCVNLTTRTQLPPAYTNSFTRGVYYPDKVFRSSVLHSTQDLFLPFFSNVTWFHA
IHVSGTNGTKRFDNPVLPFNDGVYFASTEKSNIIRGWIFGTTLDSKTQSLLIVNNATNVVIKVCEFQF
CNDPFLGVYYHKNNKSWMESEFRVYSSANNCTFEYVSQPFLMDLEGKQGNFKNLREFVFKNIDGY
FKIYSKHTPINLVRDLPQGFSALEPLVDLPIGINITRFQTLLALHRSYLTPGDSSSGWTAGAAAYYVG
YLQPRTFLLKYNENGTITDAVDCALDPLSETKCTLKSFTVEKGIYQTSNFRVQPTESIVRFPNITNLCP
FGEVFNATRFASVYAWNRKRISNCVADYSVLYNSASFSTFKCYGVSPTKLNDLCFTNVYADSFVIR
GDEVRQIAPGQTGKIADYNYKLPDDFTGCVIAWNSNNLDSKVGGNYNYLYRLFRKSNLKPFERDIS
TEIYQAGSTPCNGVEGFNCYFPLQSYGFQPTNGVGYQPYRVVVLSFELLHAPATVCGPKKSTNLVK
NKCVNFNFNGLTGTGVLTESNKKFLPFQQFGRDIADTTDAVRDPQTLEILDITPCSFGGVSVITPGTN
TSNQVAVLYQDVNCTEVPVAIHADQLTPTWRVYSTGSNVFQTRAGCLIGAEHVNNSYECDIPIGAGI
CASYQTQTNSP**AAAA**SVASQSIIAYTMSLGAENSVAYSNNSIAIPTNFTISVTTEILPVSMTKTSVDCT
MYICGDSTECSNLLLQYGSFCTQLNRALTGIAVEQDKNTQEVFAQVKQIYKTPPIKDFGGFNFSQILP
DPSKPS**GH**SFIEDLLFNKVTLADAGFIKQYGDCLGDIAARDLICAQKFNGLTVLPPLLTDEMIAQYTS
ALLAGTITSGWTFGAGAALQIPFAMQMAYRFNGIGVTQNVLYENQKLIANQFNSAIGKIQDSLSSTA
SALGKLQDVVNQNAQALNTLVKQLSSNFGAISSVLNDILSRLDKVEAEVQIDRLITGRLQSLQTYVT
QQLIRAAEIRASANLAATKMSECVLGQSKRVDFCGKGYHLMSFPQSAPHGVVFLHVTYVPAQEKN
FTTAPAICHDGKAHFPREGVFVSNGTHWFVTQRNFYEPQIITTDNTFVSGNCDVVIGIVNNTVYDPL
QPELDSFKEELDKYFKNHTSPDVDLGDISGINASVVNIQKEIDRLNEVAKNLNESLIDLQELGKYEQY
IKWPWYIWLGFIAGLIAIVMVTIMLCCMTSCCSCLKGCCSCGSCC*DYKDHDGDYKDHDIDYKDDDD*
K (see note iii)

3.3.11 Notes

(3a) It is important to truncate the last 19–21 C-terminal amino acids of spike, which encode for an endoplasmic reticulum retention signal. This will greatly increase spike expression on the cell surface and hence enable efficient ACE2 interaction and syncytium formation. For detection purposes, we replaced these 19 C-terminal residues with a FLAG-tag. Expression plasmids encoding the different spike sequences were custom-synthesized and are available upon request. Plasmids encoding HiBiT and LgBiT can be purchased from Promega.

(3b) Mutations, insertions or deletions in the spike variants, in respect to the original Wuhan variant, are depicted in red and in bold,

underlined or _ respectively. The C-terminal FLAG-tag that replaces the last 19 amino acids of spike (KFDEDDSEPVLKGVKLHYT) is depicted in italic letters.

(3c) This spike variant has an impaired S1/S2 furin cleavage site as well as an impaired TMPRSS2 S2' cleavage site (Hornich et al., 2021). Surface expression of this variant is comparable to WT spike, but its ability to induce syncytia is abolished, thus serving as appropriate negative control to normalize to 0% cell fusion.

4. Step-by-step method details

The following protocol uses HEK293T cells transiently transfected to express the spike protein and LgBiT and Vero E6 cells endogenously expressing ACE2 receptor transiently transfected to express HiBiT. As explained in the materials section "cell culture and transfection," the selection of the correct cell line is crucial and different alternatives exist to choose between transient transfections and stably expressing cells.

4.1 Cell preparation and transfection

The protocol described below should be performed in sterile conditions under a laminar flow hood. Cell lines and patient samples are to be handled according to the biosafety regulations of each facility/country.

1. Maintain HEK293T and Vero E6 cells in culture medium (we recommend DMEM supplemented with 10% FBS and 100 units/mL of penicillin and 100 μg/mL of streptomycin) at 37 °C with 5% CO_2.
2. Seed 100,000 HEK293T cells/cm^2 and 50,000 Vero E6 cells/cm^2 in separate 10-cm cell culture dishes with 10 mL of culture medium (see note 4b). Be aware that at least two 10-cm cell culture dishes will be required for HEK293T cells (see note 4d).
3. Incubate the cells at 37 °C with 5% CO_2 for 24 h.
4. For Vero E6 cells: Dilute 18 μL of PEI in 600 μL of Opti-MEM. In a separate tube, add 6 μg HiBiT-encoding vector to 600 μL of Opti-MEM and mix thoroughly.
5. For HEK293T cells: Dilute 9 μL of PEI in 300 μL of Opti-MEM. In a separate tube, add 2.9 μg LgBiT-encoding vector and 150 ng SARS-CoV-2 spike-encoding vector in 300 μL of Opti-MEM and mix thoroughly (see note 4a, 4c and 4d).
6. Add the PEI-Opti-MEM mix to the DNA and mix gently by pipetting up and down.

7. Incubate the mix for 20 min at room temperature.
8. During this period, remove the medium from the dishes and add 10 mL of fresh pre-warmed culture medium.
9. Add the mix to the cells in a dropwise manner and ensure even distribution over the surface.
10. Incubate the cells at 37 °C with 5% CO_2 for 24 h.

4.1.1 Notes

4a. All plasmids encoding for the different C-truncated spike variants are available upon request (andy.chevigne@lih.lu).

4b. Cell density was optimized for HEK293T and Vero E6 but other cell lines can be used. Other cell culture vessels may be used with adapted medium volumes, transfection mixes and the DNA:PEI ratio of 3:1 (w/w) maintained.

4c. Different ratios between LgBiT and HiBiT as well as the amount of spike-encoding DNA to be transfected have been tested. In our hands, the concentrations indicated above yielded consistent results, with signal-to-noise ratios regularly over 1000. Note that the amount of transfected spike-encoding DNA is very low compared to LgBiT and HiBIT sensors. In our hands, this amount ensures efficient/proper syncytium formation, while keeping low spike surface level, thus ensuring efficient neutralization, even by sera containing low amounts of neutralizing antibodies.

4d. Besides a dish with HEK293T cells transfected with DNA encoding LgBiT together with a fusion-competent spike variant, one additional 10-cm cell culture dish is required to express LgBiT together with a negative control protein as for example a fusion-deficient spike variant (see previous section spike "DEAD"), which will be used afterwards to normalize to 0% cell fusion or 100% inhibition of fusion (see section about "expected outcome and quantification").

4.2 Neutralization assay performance and reading

1. For spike and LgBiT-expressing HEK293T cells (hereafter called HEK-S-LgBiT): Aspirate the culture medium and wash the cells with PBS.
2. Add 1 mL Versene to each dish and incubate at 37 °C for 5 min (see note 4e).
3. Collect HEK-S-LgBiT cells in culture medium and transfer them to a 15-mL conical tube.

4. Count the cells and centrifuge them for 5 min at 300 x *g* at room temperature.
5. Discard the supernatant and resuspend the cells in culture medium at a concentration of 1×10^6 cells/mL.
6. In a transparent U-bottom 96-well plate, prepare the sera and/or other samples and dilutions to be tested at a 2x final concentration in 26 µL culture medium per condition.
7. With a multichannel pipet, add 26 µL HEK-S-LgBiT cells to the 26 µL sera dilutions and mix by pipetting several times up and down (these volumes are sufficient for a technical duplicate in a 96-well format (see note 4f)).
8. Incubate the cells with serum for 60 min at 37 °C and 5% CO_2.
9. In the meantime, detach and resuspend HiBiT- and ACE2-expressing Vero E6 cells (hereafter called Vero-ACE2-HiBiT cells). For this, repeat the procedure as described in steps 1–5 of this section.
10. With a multichannel pipet, distribute 60 µL Vero-ACE2-HiBiT cells per well of a white 96-well plate.
11. With a multichannel pipet, transfer 20 µL of serum-incubated HEK-S-LgBiT cells to the 60 µL Vero-ACE2-HiBiT cells in the white 96-well plate. Mix thoroughly by pipetting up and down. The initial volume of 52 µL (26 µL serum + 26 µL HEK-S-LgBiT cells) allows pipetting a technical duplicate using twice 20 µL of serum/HEK cell mix.
12. Put a lid on the 96-well plate and incubate for 16–20 h at 37 °C 5% CO_2 (see note 4g).

As a recapitulation, each well should contain 60,000 Vero-ACE2-HiBiT cells and 10,000 serum-preincubated HEK-S-LgBiT cells in a total volume of 80 µL.

13. After 16–20 h incubation, discard the medium either carefully with a multichannel pipet or by firmly inverting the plate over a safe reservoir/bin (the cells will remain adhered).
14. With a multichannel pipet, add 100 µL of NanoLuc® substrate prepared according to the kit's instructions (see note 4h) and directly read the luminescence with a plate reader for 20 min.
15. Analyze the data considering the different possibilities presented in the section "expected outcome and quantification."

4.2.1 Notes

4e Proteolytic priming of the spike protein is a prerequisite for coronavirus entry into host cells and syncytia formation. This priming event can be

mediated by host cell proteases such as Furin and TMPRSS2 but also by Trypsin, as shown (Ou et al., 2020; Xia et al., 2020). Detaching the cells with Trypsin will thus prime the spike protein on the cell surface, leading to an increase in syncytium formation upon mixing with ACE2-expressing cells (Kim et al., 2022). Although this step further increases the signal-to-noise ratio for cell fusion, in our hands, it decreases the sensitivity for antibody neutralization assays, probably due to a higher proportion of active spike protein that is harder to neutralize with antibodies.

4f The assay can be equally well performed in a 96-well, as well as in a 384-well format for high-throughput purposes. Even though the raw luminescent signal will be lower in 384-well format, the overall sensitivity is barely impacted and antibody titrations yield very similar results in both formats (see Fig. 2). In our hands, a two-fold reduction of all volumes throughout the assay compared to 96-well format yielded

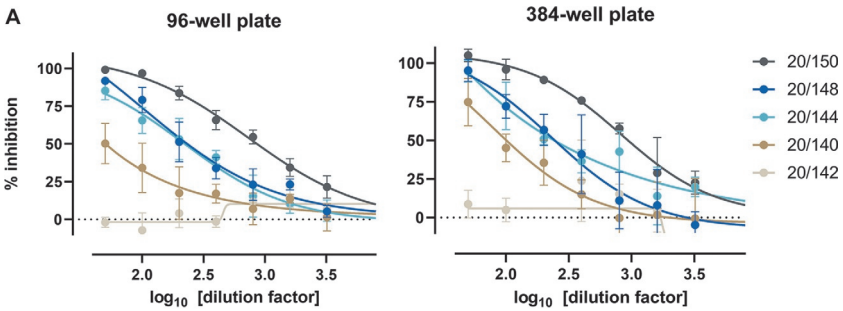

B

	WHO Reference Panel 20/268					
serum reference	20/150	20/148	20/144	20/140	20/142	
antibody level	High	Mid	low S, high N	Low	Neg.	
neutralizing antibodies	1473	210	95	44	/	IU/ml
anti-Spike IgG	832	241	86	53	/	BAU/ml
anti-N IgG	713	295	146	12	/	BAU/ml
NT_{50} 96-well plate	732	225	213	52	/	fold dil.
NT_{50} 384-well plate	820	230	222	77	/	fold dil.

Fig. 2 Neutralizing antibody titration in 96- and 384-well format. (A) Titration of the first WHO International Reference Panel for anti-SARS-CoV-2 immunoglobulin (NIBSC code: 20/268) in an assay performed in 96- or 384-well format. (B) Comparison of NT_{50} (dilution factor leading to 50% inhibition of syncytium formation) determined in either 96- or 384-well format for WHO reference sera (20/150, 20/148, 20/144, 20/140 and 20/142) containing different levels of neutralizing antibodies (in international units, IU) and spike- and nucleocapsid (N)-binding antibodies (in binding antibody units, BAU).

the best results for working in a 384-well format (i.e. mixing 13 μL HEK-S-LgBiT with 13 μL serum (step 7) and transferring 10 μL of serum/HEK-S-LgBiT cell mix to 30 μL Vero-ACE2-HiBIT cells (steps 10 and 11), leading to 30,000 Vero cells and 5,000 HEK cells in 40 μL per well of a 384-well plate).

4g Shorter incubation times are possible but might lead to higher fluctuations in signal-to-noise ratio. Optimal incubation times also depend on the spike variant to be analyzed (e.g. Delta variant generates quicker and larger syncytia than WT for example, see Fig. 5B).

4h We highly recommend to use Furimazine as substrate, which is included in several detection kits from Promega such as Nano-Glo Live Cell Assay System. Other substrates, such as coelenterazine H diluted to a final concentration of 10 nM in Opti-MEM will generate a reliable albeit reduced signal. However, coelenterazine H is prone to chemical instability, primarily through auto-oxidation, which may generate a higher background luminescence and decrease the sensitivity of the assay as well as a quicker drop in signal intensity over time.

4.3 Optional steps

As indicated in the section "before you begin," the assay can easily be adapted to different circulating spike variants, as well as potential new variants that might emerge in the future. If the assay is performed by transiently transfecting plasmids encoding for spike protein, several dishes with HEK cells can be transfected in parallel with the different spike variants of interest, allowing a deeper comparison of the neutralization profile of given sera against chosen variants of concern (see Fig. 3). In our hands, expression levels in HEK293T cells transiently transfected with same amounts of encoding DNA were almost identical for all spike variants tested so far. Alternatively, different stable cell lines expressing the spike variants may also be considered. However, in order to properly compare the neutralization profile of sera against different variants, it is crucial to verify that the different cell lines express similar levels of the spike variants.

Note that the assay works significantly less well for the Omicron spike variant. This is due to its different entry mechanism that has a greater dependency on endocytic pathways, requiring the activity of endosomal cathepsins to cleave spike. In contrast, the variant is largely independent of the TMPRSS2 protease, which is mainly responsible for inducing plasma membrane fusion (Du et al., 2022; Meng et al., 2022; Zhao et al., 2022).

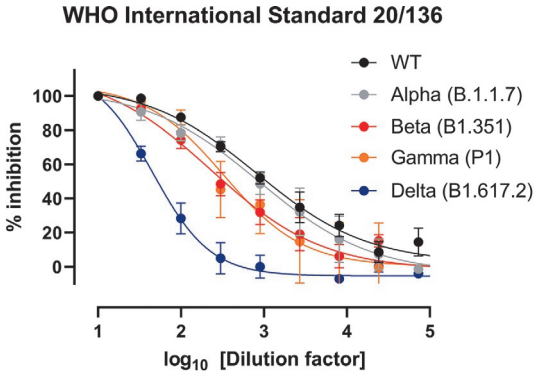

	WT	Alpha	Beta	Gamma	Delta
NT_{50}	827	868	272	330	46

Fig. 3 Neutralizing antibody titration on different spike variants. Titration of the first WHO International Standard for anti-SARS-CoV-2 immunoglobulin (NIBSC code: 20/136, having an assigned potency of 1000 IU/mL for neutralizing antibody activity) against the original spike, as well as spikes from variants Alpha, Beta, Gamma and Delta. The dilution factor leading to 50% inhibition of syncytium formation (NT_{50}) for the different variants is indicated in the table. Note the three different profiles of strong neutralization for WT and Alpha, medium neutralization for Beta and Gamma and low neutralization for Delta.

This issue can partially be circumvented by increasing the amount of transfected Omicron spike-encoding plasmid (for example from the initially indicated 150 ng to 1500 ng), increasing the signal-to-noise ratio. This increased surface expression of spike however prevents a comparison of the neutralization profile of a serum between variants, as more antibodies are needed to neutralize the higher quantity of expressed surface spike. Alternatively, a different cell line overexpressing the ACE2 receptor (like the aforementioned HEK-ACE2 cell line from VectorBuilder) can also be considered to compensate the reduced syncytia formation. However, the assay can again not be compared with the neutralization profile for other spike variants, considering the different experimental set-up.

5. Expected outcome and quantification

Depending on the plate reader, the integration time and the spike variant, readings that reach above 10^8 relative light units (RLU) for non-inhibited syncytium formation are not unusual. We suggest to include

a positive control on each plate, i.e. cells that have not been treated with a serum, representing a maximal syncytium formation (or 0% inhibition). For normalization purposes, we furthermore recommend to include a negative control on each plate, representing 0% syncytium formation (or 100% inhibition). A suitable candidate for this would be HEK293T cells, co-transfected with DNA encoding LgBiT and a fusion-deficient spike variant (see note 3c, section "Sequences of NanoLuc® partners and spike expression constructs," spike "DEAD"), or an irrelevant protein of similar size. Luminescence intensity for this negative control can still reach relatively high levels due to cell-death-related NanoLuc® complementation, however, syncytium-driven NanoLuc® complementation should yield at least 100-fold, in most cases several thousand fold increase in signal compared to the negative control. We recommend including positive and negative controls in technical triplicates, spread over the multiwell plate, in order to minimize inter- and intra-plate variations.

Several options exist to normalize the data. An accurate and easy way is to express the data as "fold negative control," especially if only a few samples are to be compared. However, another method which proved very efficient in our hands is to normalize the data as percentage of inhibition (see Figs. 2–5). This procedure allows to compare multiple samples, even if their individual relative light units or "fold negative control" values greatly vary, as for example when comparing multiple spike variants on one graph (see Fig. 3). Normalization to percentage of inhibition can be done with the following formula, where *pos. control* represents the highest possible value, i.e. 0% syncytia inhibition, *neg. control* the lowest possible value, i.e. no syncytia formation or 100% inhibition and *sample* the sample to be analyzed, treated (or not) with neutralizing antibodies:

$$\left(\frac{\text{pos.control} - \text{sample}}{\text{pos.control} - \text{neg.control}}\right) * 100$$

It should be noted that the WHO, together with the National Institute for Biological Standards and Control (NIBSC) provide the scientific community with several standards and research reagents for anti-SARS-CoV-2 antibodies (Mattiuzzo et al., 2020). These include the First WHO International Standard for anti-SARS-CoV-2 immunoglobulin, NIBSC code 20/136 (see Fig. 3) to which an arbitrary potency of 1000 IU/mL for neutralizing antibody activity was assigned, as well as the first WHO International Reference Panel, NIBSC code 20/268, which includes five different

samples of varying amounts of antibodies (see Fig. 2). Several other working reagents calibrated to the first WHO Standard are furthermore available. Normalization to such standards and reference samples are of great value for inter-assay comparisons and standardization between laboratories. (Knezevic et al., 2022; Kristiansen et al., 2021; Mattiuzzo et al., 2020).

6. Advantages

This cell fusion-based assay provides a series of advantages compared to other neutralization assays. The absence of replication-competent viruses or infectious material allows to considerably lower the biosafety risk, enabling easier and faster sample handling as well as quick and cost-efficient waste disposal. This furthermore eliminates the requirement of specifically trained staff for high biosafety facilities, as all steps of the protocol can be performed in a standard cell culture facility.

This assay is also less artificial compared to cell-free assays, since the trimeric spike is exposed in its correct tridimensional conformation on a cell membrane, allowing a closer reproduction of the viral encounter with neutralizing antibodies. This enables to also detect neutralizing antibodies that recognize more complex and conformational epitopes, that would be overlooked/missed using cell-free assays based on monomeric spike for example.

Building on state-of-the-art high-affinity NanoLuc® complementation, the assay is extremely sensitive, resulting in an excellent signal-to-noise ratio and high reproducibility. The determined NT_{50} values for the WHO Standard and WHO Reference Panel are well in line with reported values from other laboratories using live virus neutralization assays (compare Figs. 2 and 3 with (Mattiuzzo et al., 2020)). The assay can be easily performed in a 96- or 384-well format, qualifying it for high-throughput purposes at a reasonably low cost. Indeed, our method has recently been applied to the CON-VINCE cohort, a nation-wide representative study for assessing SARS-CoV-2-spread in the Luxembourgish population. In this context, sera of over 1300 participants were screened for neutralizing antibodies within one week by a single experimenter (see Fig. 4) (Snoeck et al., 2020).

Lastly, the assay can easily be applied to new emerging SARS-CoV-2 variants, allowing to quickly adapt to upcoming needs and compare the neutralization profile of antibodies towards different variants.

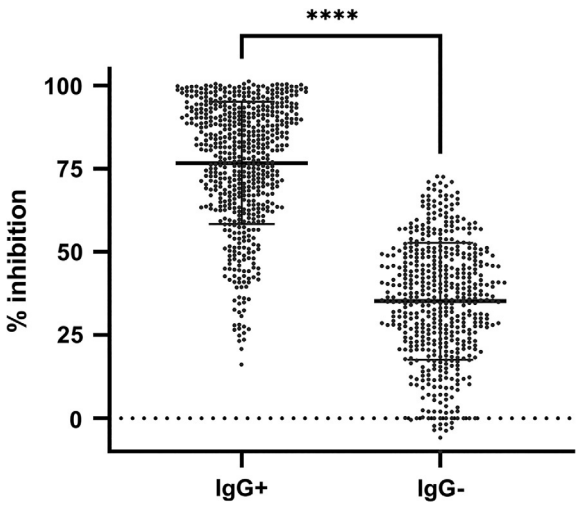

Fig. 4 Example of high-throughput characterization of sera from over 1300 subjects. Sera from SARS-CoV-2-negative, asymptomatic or mildly symptomatic individuals analyzed by two commercial kits (EuroImmun and Meso Scale Diagnostics) for the presence of SARS-CoV-2 spike IgG were blind tested in the described cell fusion assay for neutralizing antibodies. Inhibition of syncytia formation was then stratified according to IgG positive/negative status. **** $P < 0.0001$ by two tailed Mann-Whitney test.

7. Limitations

Although the assay provides a lot of advantages, it should be noted that replication-competent full-length virus neutralization in a BSL3 facility remains the gold standard. Although spike expression can easily be verified on the cell surface, the absolute amount of spike protein per cell is likely to be much higher than on a viral particle and expression is hard to quantify and to control. If a transient transfection protocol is chosen, fluctuations in transfection efficacy and cell fitness might lead to variations of the results. Hence, it is important to include in every run adequate controls like the aforementioned spike "DEAD" and/or the standards provided by the WHO and NIBSC.

8. Alternative methods/procedures

Besides changing spike variants to determine different neutralization profiles of antibodies, one alternative step in the assay preparation can be considered: Instead of freshly adding furimazine substrate to determine syncytia formation after the 16–20 h incubation step at 37 °C, 5% CO_2 (step 14 section "Neutralization assay performance and reading"), the cells can be

incubated in advance with an Extended Live Cell substrate, such as Endurazine™ or Vivazine™. For this, simply add one of these substrates to the Vero-ACE2-HiBiT cells to a final dilution of 1:100 before distributing 60 µL per well of a white 96-well plate (before step 10 section "Neutralization assay performance and reading"). Nano-Glo Endurazine™ and Vivazine™ are modified versions of furimazine which are hydrolyzed at slow rate by cellular esterases, hence releasing active furimazine throughout the experiment for several hours or days. Pre-loading the cells with one of these substrates with prolonged lifetime allows to read the plate after the 16–20 h incubation step, without having to perform a washing step or having to freshly add NanoLuc® substrate (see Fig. 5A). This reduces pipetting steps and hence well-to-well

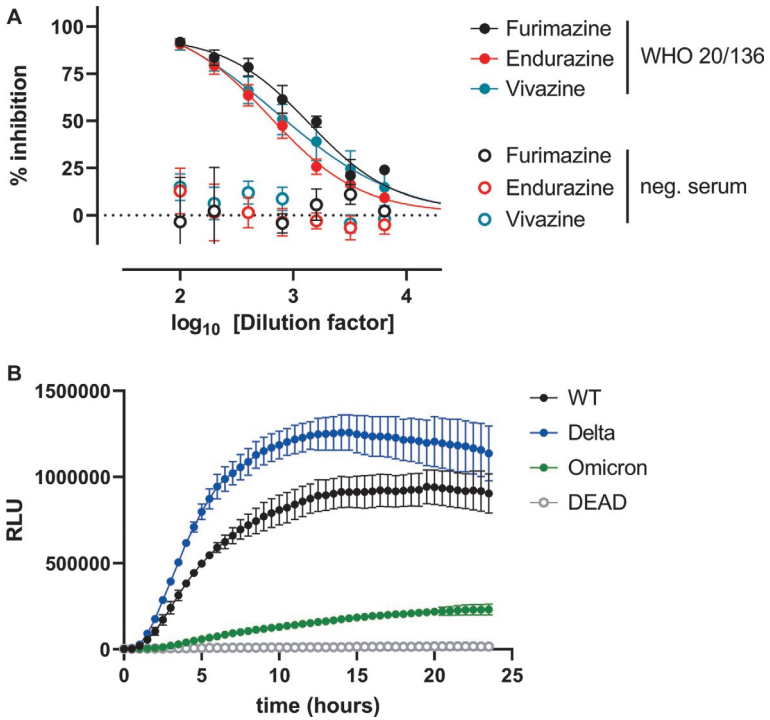

Fig. 5 Use of alternative NanoLuc® substrates with prolonged lifetime. (A) Comparison between classical furimazine and Extended Life Cell substrates Endurazine™ and Vivazine™. Cells were either treated with increasing concentrations of WHO standard 20/136, or with a negative control serum. While furimazine was freshly added to the cells immediately before reading, Endurazine™ or Vivazine™ were incubated for 16–20 h before the measurement as described in section "alternative methods/procedures." (B) Kinetics of syncytium formation for spike WT, Delta, Omicron or a fusion-deficient spike (DEAD). Cells were incubated with Endurazine™ and luminescence was measured once every 30 min over 24 h. Note that a ten times higher amount of spike was transfected for Omicron variant, in order to enhance its low syncytium formation ability.

fluctuations and facilitates automatization of the reading, since no manual steps are to be performed after mixing both cell lines in a 96-well plate.

The use of these substrates also allows to study kinetics of syncytium formation. For this, the cells can be similarly pre-loaded with substrate and luminescence read over time, instead of an end-point measurement after 16–20 h incubation (see Fig. 5B). Ensure that the cells are kept over the entire reading period at 37 °C and 5% CO_2, or, if not possible, in a CO_2-independent buffer, like 20 mM HEPES.

Lastly, in addition to high-throughput screening of neutralizing SARS-CoV-2 antibodies detailed in this protocol, the assay is similarly applicable to high-throughput drug screenings targeting the ACE2, TMPRSS2, spike or the fusion process itself.

Acknowledgments

This study was supported by the Luxembourg Institute of Health (LIH), Laboratoires Réunis Luxembourg, the Luxembourg National Research Fund for BRIDGES Nanolux SARS-CoV-2 (BRIDGES2020/BM/14817317) and for CONVINCE 14716281/CON-VINCE/Krueger together with the André Losch Foundation. The authors wish to thank the members of CON-VINCE Consortium (https://cloud.lih.lu/s/KrSow4aqAXGZAXB), Manuel Counson, Nadia Beaupain, Tomasz Uchański and Christie B. Palmer for technical help, scientific support and figure design.

References

Almahboub, S. A., Algaissi, A., Alfaleh, M. A., ElAssouli, M. Z., & Hashem, A. M. (2020). Evaluation of neutralizing antibodies against highly pathogenic coronaviruses: A detailed protocol for a rapid evaluation of neutralizing antibodies using vesicular stomatitis virus pseudovirus-based assay. *Frontiers in Microbiology*, *11*, 2020. https://doi.org/10.3389/fmicb.2020.02020.

Bewley, K. R., Coombes, N. S., Gagnon, L., McInroy, L., Baker, N., Shaik, I., et al. (2021). Quantification of SARS-CoV-2 neutralizing antibody by wild-type plaque reduction neutralization, microneutralization and pseudotyped virus neutralization assays. *Nature Protocols*, *16*(6), 3114–3140. https://doi.org/10.1038/s41596-021-00536-y.

Buchrieser, J., Dufloo, J., Hubert, M., Monel, B., Planas, D., Rajah, M. M., et al. (2021). Syncytia formation by SARS-CoV-2-infected cells. *The EMBO Journal*, *40*(3), e107405. https://doi.org/10.15252/embj.2020107405.

Cai, W., Tang, Z. M., Wen, G. P., Wang, S. L., Ji, W. F., Yang, M., et al. (2016). A high-throughput neutralizing assay for antibodies and sera against hepatitis E virus. *Scientific Reports*, *6*, 25141. https://doi.org/10.1038/srep25141.

Case, J. B., Rothlauf, P. W., Chen, R. E., Liu, Z., Zhao, H., Kim, A. S., et al. (2020). Neutralizing antibody and soluble ACE2 inhibition of a replication-competent VSV-SARS-CoV-2 and a clinical isolate of SARS-CoV-2. *Cell Host & Microbe*, *28*(3), 475–485 e475. https://doi.org/10.1016/j.chom.2020.06.021.

Chan, J. F., Kok, K. H., Zhu, Z., Chu, H., To, K. K., Yuan, S., et al. (2020). Genomic characterization of the 2019 novel human-pathogenic coronavirus isolated from a patient with atypical pneumonia after visiting Wuhan. *Emerging Microbes & Infections*, *9*(1), 221–236. https://doi.org/10.1080/22221751.2020.1719902.

Cucinotta, D., & Vanelli, M. (2020). WHO declares COVID-19 a pandemic. *Acta-Biomedica*, *91*(1), 157–160. https://doi.org/10.23750/abm.v91i1.9397.

Danh, K., Karp, D. G., Robinson, P. V., Seftel, D., Stone, M., Simmons, G., et al. (2020). Detection of SARS-CoV-2 neutralizing antibodies with a cell-free PCR assay. *medRxiv*. https://doi.org/10.1101/2020.05.28.20105692.

Dejnirattisai, W., Shaw, R. H., Supasa, P., Liu, C., Stuart, A. S., Pollard, A. J., et al. (2022). Reduced neutralisation of SARS-CoV-2 omicron B.1.1.529 variant by post-immunisation serum. *Lancet*, *399*(10321), 234–236. https://doi.org/10.1016/S0140-6736(21)02844-0.

Deshpande, G. R., Sapkal, G. N., Tilekar, B. N., Yadav, P. D., Gurav, Y., Gaikwad, S., et al. (2020). Neutralizing antibody responses to SARS-CoV-2 in COVID-19 patients. *The Indian Journal of Medical Research*, *152*(1 & 2), 82–87. https://doi.org/10.4103/ijmr.IJMR_2382_20.

Dixon, A. S., Schwinn, M. K., Hall, M. P., Zimmerman, K., Otto, P., Lubben, T. H., et al. (2016). NanoLuc complementation reporter optimized for accurate measurement of protein interactions in cells. *ACS Chemical Biology*, *11*(2), 400–408. https://doi.org/10.1021/acschembio.5b00753.

Du, X., Tang, H., Gao, L., Wu, Z., Meng, F., Yan, R., et al. (2022). Omicron adopts a different strategy from Delta and other variants to adapt to host. *Signal Transduction and Targeted Therapy*, 7(1), 45. https://doi.org/10.1038/s41392-022-00903-5.

Du, L., Yang, Y., & Zhang, X. (2021). Neutralizing antibodies for the prevention and treatment of COVID-19. *Cellular & Molecular Immunology*, *18*(10), 2293–2306. https://doi.org/10.1038/s41423-021-00752-2.

Duarte, C. M., Ketcheson, D. I., Eguiluz, V. M., Agusti, S., Fernandez-Gracia, J., Jamil, T., et al. (2022). Rapid evolution of SARS-CoV-2 challenges human defenses. *Scientific Reports*, *12*(1), 6457. https://doi.org/10.1038/s41598-022-10097-z.

Fenwick, C., Turelli, P., Pellaton, C., Farina, A., Campos, J., Raclot, C., et al. (2021). A high-throughput cell- and virus-free assay shows reduced neutralization of SARS-CoV-2 variants by COVID-19 convalescent plasma. *Science Translational Medicine*, *13*(605). https://doi.org/10.1126/scitranslmed.abi8452.

Gaebler, C., Wang, Z., Lorenzi, J. C. C., Muecksch, F., Finkin, S., Tokuyama, M., et al. (2021). Evolution of antibody immunity to SARS-CoV-2. *Nature*, *591*(7851), 639–644. https://doi.org/10.1038/s41586-021-03207-w.

Hall, M. P., Unch, J., Binkowski, B. F., Valley, M. P., Butler, B. L., Wood, M. G., et al. (2012). Engineered luciferase reporter from a deep sea shrimp utilizing a novel imidazopyrazinone substrate. *ACS Chemical Biology*, 7(11), 1848–1857. https://doi.org/10.1021/cb3002478.

Han, D. P., Kim, H. G., Kim, Y. B., Poon, L. L., & Cho, M. W. (2004). Development of a safe neutralization assay for SARS-CoV and characterization of S-glycoprotein. *Virology*, *326*(1), 140–149. https://doi.org/10.1016/j.virol.2004.05.017.

Harvey, W. T., Carabelli, A. M., Jackson, B., Gupta, R. K., Thomson, E. C., Harrison, E. M., et al. (2021). SARS-CoV-2 variants, spike mutations and immune escape. *Nature Reviews. Microbiology*, *19*(7), 409–424. https://doi.org/10.1038/s41579-021-00573-0.

Herschhorn, A., Finzi, A., Jones, D. M., Courter, J. R., Sugawara, A., Smith, A. B., 3rd, et al. (2011). An inducible cell-cell fusion system with integrated ability to measure the efficiency and specificity of HIV-1 entry inhibitors. *PLoS One*, *6*(11), e26731. https://doi.org/10.1371/journal.pone.0026731.

Hoffmann, M., Kleine-Weber, H., Schroeder, S., Kruger, N., Herrler, T., Erichsen, S., et al. (2020). SARS-CoV-2 cell entry depends on ACE2 and TMPRSS2 and is blocked by a clinically proven protease inhibitor. *Cell*, *181*(2), 271–280 e278. https://doi.org/10.1016/j.cell.2020.02.052.

Hornich, B. F., Grosskopf, A. K., Schlagowski, S., Tenbusch, M., Kleine-Weber, H., Neipel, F., et al. (2021). SARS-CoV-2 and SARS-CoV spike-mediated cell-cell fusion differ in their requirements for receptor expression and proteolytic activation. *Journal of Virology*, *95*(9). https://doi.org/10.1128/JVI.00002-21.

Huang, Y., Yang, C., Xu, X. F., Xu, W., & Liu, S. W. (2020). Structural and functional properties of SARS-CoV-2 spike protein: Potential antivirus drug development for COVID-19. *Acta Pharmacologica Sinica*, *41*(9), 1141–1149. https://doi.org/10.1038/s41401-020-0485-4.

Israel, A., Shenhar, Y., Green, I., Merzon, E., Golan-Cohen, A., Schaffer, A. A., et al. (2021). Large-scale study of antibody titer decay following BNT162b2 mRNA vaccine or SARS-CoV-2 infection. *Vaccines (Basel)*, *10*(1). https://doi.org/10.3390/vaccines10010064.

Jaimes, J. A., Millet, J. K., & Whittaker, G. R. (2020). Proteolytic cleavage of the SARS-CoV-2 spike protein and the role of the novel S1/S2 site. *iScience*, *23*(6), 101212. https://doi.org/10.1016/j.isci.2020.101212.

Janaka, S. K., Clark, N. M., Evans, D. T., & Connor, J. P. (2021). Predicting the efficacy of COVID-19 convalescent plasma donor units with the lumit dx anti-receptor binding domain assay. *medRxiv*. https://doi.org/10.1101/2021.03.08.21253135.

Johnson, M., Wagstaffe, H. R., Gilmour, K. C., Mai, A. L., Lewis, J., Hunt, A., et al. (2020). Evaluation of a novel multiplexed assay for determining IgG levels and functional activity to SARS-CoV-2. *Journal of Clinical Virology*, *130*, 104572. https://doi.org/10.1016/j.jcv.2020.104572.

Kim, Y., Jang, G., Lee, D., Kim, N., Seon, J. W., Kim, Y. H., et al. (2022). Trypsin enhances SARS-CoV-2 infection by facilitating viral entry. *Archives of Virology*, *167*(2), 441–458. https://doi.org/10.1007/s00705-021-05343-0.

Knezevic, I., Mattiuzzo, G., Page, M., Minor, P., Griffiths, E., Nuebling, M., et al. (2022). WHO International Standard for evaluation of the antibody response to COVID-19 vaccines: Call for urgent action by the scientific community. *Lancet Microbe*, *3*(3), e235–e240. https://doi.org/10.1016/S2666-5247(21)00266-4.

Krah, D. L., Amin, R. D., Nalin, D. R., & Provost, P. J. (1991). A simple antigen-reduction assay for the measurement of neutralizing antibodies to hepatitis A virus. *The Journal of Infectious Diseases*, *163*(3), 634–637. https://doi.org/10.1093/infdis/163.3.634.

Kristiansen, P. A., Page, M., Bernasconi, V., Mattiuzzo, G., Dull, P., Makar, K., et al. (2021). WHO International Standard for anti-SARS-CoV-2 immunoglobulin. *Lancet*, *397*(10282), 1347–1348. https://doi.org/10.1016/S0140-6736(21)00527-4.

Li, G., Fan, Y., Lai, Y., Han, T., Li, Z., Zhou, P., et al. (2020). Coronavirus infections and immune responses. *Journal of Medical Virology*, *92*(4), 424–432. https://doi.org/10.1002/jmv.25685.

Liu, L., Wang, P., Nair, M. S., Yu, J., Rapp, M., Wang, Q., et al. (2020). Potent neutralizing antibodies against multiple epitopes on SARS-CoV-2 spike. *Nature*, *584*(7821), 450–456. https://doi.org/10.1038/s41586-020-2571-7.

Luís, R., D'Uonnolo, G., Palmer, C. B., Meyrath, M., Uchański, T., Wantz, M., et al. (2022). Chapter 13—Nanoluciferase-based methods to monitor activation, modulation and trafficking of atypical chemokine receptors. In A. K. Shukla (Ed.), *Vol. 169. Methods in Cell Biology* (pp. 279–294). Academic Press.

Marin, M., Du, Y., Giroud, C., Kim, J. H., Qui, M., Fu, H., et al. (2015). High-throughput HIV-cell fusion assay for discovery of virus entry inhibitors. *Assay and Drug Development Technologies*, *13*(3), 155–166. https://doi.org/10.1089/adt.2015.639.

Mattiuzzo, G., Bentley, E. M., Hassall, M., Routley, S., Richardson, S., Bernasconi, V., et al. (2020). *Establishment of the WHO International Standard and Reference Panel for anti-SARS-CoV-2 antibody (WHO/BS/2020/2403)*. World Health Organization.

Meng, B., Abdullahi, A., Ferreira, I., Goonawardane, N., Saito, A., Kimura, I., et al. (2022). Altered TMPRSS2 usage by SARS-CoV-2 Omicron impacts tropism and fusogenicity. *Nature*. https://doi.org/10.1038/s41586-022-04474-x.

Mravinacova, S., Jonsson, M., Christ, W., Klingstrom, J., Yousef, J., Hellstrom, C., et al. (2022). A cell-free high throughput assay for assessment of SARS-CoV-2 neutralizing antibodies. *New Biotechnology*, *66*, 46–52. https://doi.org/10.1016/j.nbt.2021.10.002.

Nie, J., Li, Q., Wu, J., Zhao, C., Hao, H., Liu, H., et al. (2020). Quantification of SARS-CoV-2 neutralizing antibody by a pseudotyped virus-based assay. *Nature Protocols*, *15*(11), 3699–3715. https://doi.org/10.1038/s41596-020-0394-5.

Ou, X., Liu, Y., Lei, X., Li, P., Mi, D., Ren, L., et al. (2020). Characterization of spike glycoprotein of SARS-CoV-2 on virus entry and its immune cross-reactivity with SARS-CoV. *Nature Communications*, *11*(1), 1620. https://doi.org/10.1038/s41467-020-15562-9.

Palmer, C. B., D'Uonnolo, G., Luís, R., Meyrath, M., Uchański, T., Chevigné, A., et al. (2022). Chapter 15—Nanoluciferase-based complementation assay for systematic profiling of GPCR–GRK interactions. In A. K. Shukla (Ed.), *Vol. 169. Methods in Cell Biology* (pp. 309–321). Academic Press.

Piccoli, L., Park, Y. J., Tortorici, M. A., Czudnochowski, N., Walls, A. C., Beltramello, M., et al. (2020). Mapping neutralizing and immunodominant sites on the SARS-CoV-2 spike receptor-binding domain by structure-guided high-resolution serology. *Cell*, *183*(4), 1024–1042 e1021. https://doi.org/10.1016/j.cell.2020.09.037.

Rockx, B., Corti, D., Donaldson, E., Sheahan, T., Stadler, K., Lanzavecchia, A., et al. (2008). Structural basis for potent cross-neutralizing human monoclonal antibody protection against lethal human and zoonotic severe acute respiratory syndrome coronavirus challenge. *Journal of Virology*, *82*(7), 3220–3235. https://doi.org/10.1128/JVI.02377-07.

Sarzotti-Kelsoe, M., Daniell, X., Todd, C. A., Bilska, M., Martelli, A., LaBranche, C., et al. (2014). Optimization and validation of a neutralizing antibody assay for HIV-1 in A3R5 cells. *Journal of Immunological Methods*, *409*, 147–160. https://doi.org/10.1016/j.jim.2014.02.013.

Saunders, N., Planas, D., Bolland, W. H., Rodriguez, C., Fourati, S., Buchrieser, J., et al. (2022). Fusogenicity and neutralization sensitivity of the SARS-CoV-2 delta sublineage AY.4.2. *eBioMedicine*, 77, 103934. https://doi.org/10.1016/j.ebiom.2022.103934.

Sehr, P., Rubio, I., Seitz, H., Putzker, K., Ribeiro-Muller, L., Pawlita, M., et al. (2013). High-throughput pseudovirion-based neutralization assay for analysis of natural and vaccine-induced antibodies against human papillomaviruses. *PLoS One*, *8*(10), e75677. https://doi.org/10.1371/journal.pone.0075677.

Sha, Y., Wu, Y., Cao, Z., Xu, X., Wu, W., Jiang, D., et al. (2006). A convenient cell fusion assay for the study of SARS-CoV entry and inhibition. *IUBMB Life*, *58*(8), 480–486. https://doi.org/10.1080/15216540600820974.

Snoeck, C. J., Vaillant, M., Abdelrahman, T., Satagopam, V. P., Turner, J. D., Beaumont, K., et al. (2020). Prevalence of SARS-CoV-2 infection in the Luxembourgish population—The CON-VINCE study. *medRxiv*. https://doi.org/10.1101/2020.05.11.20092916. 2020.2005.2011.20092916.

Theuerkauf, S. A., Michels, A., Riechert, V., Maier, T. J., Flory, E., Cichutek, K., et al. (2021). Quantitative assays reveal cell fusion at minimal levels of SARS-CoV-2 spike protein and fusion from without. *iScience*, *24*(3), 102170. https://doi.org/10.1016/j.isci.2021.102170.

Vacharathit, V., Srichatrapimuk, S., Manopwisedjaroen, S., Kirdlarp, S., Srisaowakarn, C., Setthaudom, C., et al. (2021). SARS-CoV-2 neutralizing antibodies decline over one year and patients with severe COVID-19 pneumonia display a unique cytokine profile. *International Journal of Infectious Diseases*, *112*, 227–234. https://doi.org/10.1016/j.ijid.2021.09.021.

Wajnberg, A., Amanat, F., Firpo, A., Altman, D. R., Bailey, M. J., Mansour, M., et al. (2020). Robust neutralizing antibodies to SARS-CoV-2 infection persist for months. *Science*, *370*(6521), 1227–1230. https://doi.org/10.1126/science.abd7728.

Walls, A. C., Park, Y. J., Tortorici, M. A., Wall, A., McGuire, A. T., & Veesler, D. (2020). Structure, function, and antigenicity of the SARS-CoV-2 spike glycoprotein. *Cell*, *183*(6), 1735. https://doi.org/10.1016/j.cell.2020.11.032.

Walls, A. C., Tortorici, M. A., Snijder, J., Xiong, X., Bosch, B. J., Rey, F. A., et al. (2017). Tectonic conformational changes of a coronavirus spike glycoprotein promote membrane fusion. *Proceedings of the National Academy of Sciences of the United States of America*, *114*(42), 11157–11162. https://doi.org/10.1073/pnas.1708727114.

Wilmes, P., Zimmer, J., Schulz, J., Glod, F., Veiber, L., Mombaerts, L., et al. (2021). SARS-CoV-2 transmission risk from asymptomatic carriers: Results from a mass screening programme in Luxembourg. *The Lancet Regional Health. Europe*, *4*, 100056. https://doi.org/10.1016/j.lanepe.2021.100056.

Wrapp, D., Wang, N., Corbett, K. S., Goldsmith, J. A., Hsieh, C. L., Abiona, O., et al. (2020). Cryo-EM structure of the 2019-nCoV spike in the prefusion conformation. *Science*, *367*(6483), 1260–1263. https://doi.org/10.1126/science.abb2507.

Xia, S., Lan, Q., Su, S., Wang, X., Xu, W., Liu, Z., et al. (2020). The role of furin cleavage site in SARS-CoV-2 spike protein-mediated membrane fusion in the presence or absence of trypsin. *Signal Transduction and Targeted Therapy*, *5*(1), 92. https://doi.org/10.1038/s41392-020-0184-0.

York, J., & Nunberg, J. H. (2018). A cell-cell fusion assay to assess arenavirus envelope glycoprotein membrane-fusion activity. *Methods in Molecular Biology*, *1604*, 157–167. https://doi.org/10.1007/978-1-4939-6981-4_10.

Zhao, G., Du, L., Ma, C., Li, Y., Li, L., Poon, V. K., et al. (2013). A safe and convenient pseudovirus-based inhibition assay to detect neutralizing antibodies and screen for viral entry inhibitors against the novel human coronavirus MERS-CoV. *Virology Journal*, *10*, 266. https://doi.org/10.1186/1743-422X-10-266.

Zhao, H., Lu, L., Peng, Z., Chen, L. L., Meng, X., Zhang, C., et al. (2022). SARS-CoV-2 Omicron variant shows less efficient replication and fusion activity when compared with delta variant in TMPRSS2-expressed cells. *Emerging Microbes & Infections*, *11*(1), 277–283. https://doi.org/10.1080/22221751.2021.2023329.

Zhao, M., Su, P. Y., Castro, D. A., Tripler, T. N., Hu, Y., Cook, M., et al. (2021). Rapid, reliable, and reproducible cell fusion assay to quantify SARS-Cov-2 spike interaction with hACE2. *PLoS Pathogens*, *17*(6), e1009683. https://doi.org/10.1371/journal.ppat.1009683.

Zhu, Z., Chakraborti, S., He, Y., Roberts, A., Sheahan, T., Xiao, X., et al. (2007). Potent cross-reactive neutralization of SARS coronavirus isolates by human monoclonal antibodies. *Proceedings of the National Academy of Sciences of the United States of America*, *104*(29), 12123–12128. https://doi.org/10.1073/pnas.0701000104.

Zou, J., Xia, H., Xie, X., Kurhade, C., Machado, R. R. G., Weaver, S. C., et al. (2022). Neutralization against Omicron SARS-CoV-2 from previous non-Omicron infection. *Nature Communications*, *13*(1), 852. https://doi.org/10.1038/s41467-022-28544-w.